Chemical Physics Letters 460 (2008) 237–240

Contents lists available at ScienceDirect

Chemical Physics Letters

journal homepage: www.elsevier.com/locate/cplett

Vibrational analysis of per-fluorinated-triamantane

Judy N. Hart [a], Paul W. May [a,*], Neil L. Allan [a], Jeremy E.P. Dahl [b], Shenggao Liu [b], Robert M.K. Carlson [b], Jamie L. Adcock [c]

[a] School of Chemistry, University of Bristol, Bristol BS8 1TS, UK
[b] Molecular Diamond Technologies, Chevron Technology Ventures, P.O. Box 1627, Richmond, CA 94802, USA
[c] The University of Tennessee, Knoxville, Tennessee 37996-1600, USA

ARTICLE INFO

Article history:
Received 19 March 2008
In final form 5 June 2008
Available online 11 June 2008

ABSTRACT

Triamantane was isolated from petroleum, per-fluorinated and the vibrational behaviour investigated by experimental and theoretical methods. Close agreement was found between the experimental and calculated Raman spectrum. The surface vibrational modes are shifted to lower wavenumbers relative to hydrogenated triamantane, due to the increased mass of the surface groups. The Raman spectrum of the fluorinated molecule more closely resembles that of pure diamond compared with hydrogenated triamantane. The absence of a peak at 1150 cm^{-1} for fluorinated triamantane suggests that this peak, often seen in the spectrum of nanocrystalline diamond, cannot be attributed to vibrations of diamond nanocrystals.

1. Introduction

Large diamondoid hydrocarbons are rigid cage-structured molecules with unusual chemical and physical properties. They are of interest both in their own right, as components of petroleum, and also for various applications including seed crystals for the chemical vapour deposition of diamond [1], building blocks for high temperature polymers [2] and field emitters [3,4]. These molecules are effectively H-terminated nanocrystals of diamond, approximately 1–2 nm in size, so their study assists in the interpretation of experimental results for nanocrystalline diamond, such as the assignment of peaks in Raman spectra [5].

The properties of these diamondoid molecules can be altered by the substitution of hydrogen by various functional groups [6,7]. An understanding of the effects of these substitutions on the properties of the molecules can be very useful for understanding, not only their chemistry, but also the behaviour of nanocrystalline diamond. In particular, it is important in the characterization of nanocrystalline diamond to be able to distinguish between vibrations associated with the nanocrystals themselves and those associated with grain boundary and surface structures. It has been previously suggested [5] that increasing the mass of the surface groups of diamondoid molecules results in vibrational behaviour similar to that of single diamond nanocrystals. Thus, it is interesting to determine the changes in the vibrational behaviour of diamondoid molecules that occur as the mass of the surface groups is increased, because this can assist in understanding the vibrational behaviour of nanocrystalline diamond. The vibrational analysis of adamantane ($C_{10}H_{16}$) in which the hydrogens were fully substituted for fluorines ($C_{10}F_{16}$) has been previously reported [8]. This is now extended to the study of the fully fluorinated larger diamondoid molecule, triamantane ($C_{18}F_{24}$, Fig. 1), henceforth termed F-triamantane. The use of theoretical calculations of the vibrational behaviour of diamondoid molecules has been found to be very helpful in the interpretation of experimental results [7,8], so a combination of experimental and theoretical techniques has been used in this work.

2. Experimental and computational methods

Triamantane [9,10] was isolated from <345 °C (atmospheric-equivalent boiling point) distillate cuts taken from gas condensate feed stocks and under conditions previously described [6]. It was then recrystallised from acetone to a purity of 99+% as determined by gas chromatographic–mass spectrometric methods [6]. The purified triamantane (1.0 g) was then triturated with 10.0 g of 0.24 mol anhydrous sodium fluoride and placed inside a fluidised bed reactor. The reaction mixture was flushed with a flow of 50 sccm helium for 30 min and cooled to −78 °C. A flow of 2 sccm 99% fluorine (giving a 4% fluorine/helium mixture) was introduced for 18 h, after which the helium flow was gradually reduced to 4 sccm (33% F_2). After a total of ~50 h, the helium flow was shut off (100% F_2) and the reactor was heated to increase the temperature gradually to 86 °C over ~2 days. The fluorine flow was switched off and the reactor was purged with helium. The solid was extracted by a distillation technique with per-fluorohexane, resulting in the isolation of 1.4 g of F-triamantane (82% purity). The F-triamantane was purified by recrystallisation to 99% determined by GCMS.

* Corresponding author. Fax: +44 (0) 117 925 1295.
E-mail address: Paul.May@bristol.ac.uk (P.W. May).

0009-2614/$ - see front matter © 2008 Elsevier B.V. All rights reserved.
doi:10.1016/j.cplett.2008.06.011

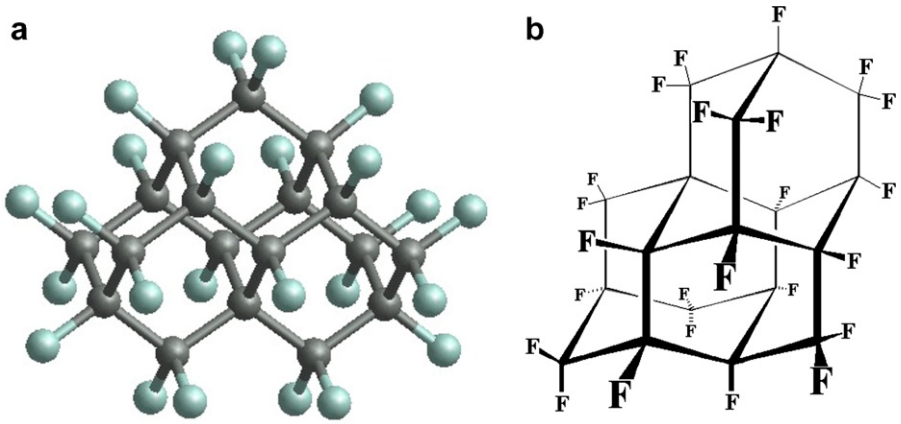

Fig. 1. Per-fluorinated triamantane (F-triamantane).

Raman spectra were acquired with a Renishaw 2000 spectrometer, using a laser excitation wavelength of 514 nm (green). Spectra were also obtained using two other laser wavelengths (UV 325 nm and near-IR 785 nm), but these provided no additional information. The crystals of F-triamantane (~0.5 mg) were placed onto a glass microscope slide, and the laser focused onto the top surface to obtain maximum signal. Spectra were recorded between 200–1400 cm^{-1}, the lower limit being determined by the cut-off filter that blocked scattered laser light. The upper limit was chosen since no peaks were observed higher than this value. The resolution of the spectrometer was ~5 cm^{-1}, and the accuracy of the wavenumber calibration across this range was ~0.5 cm^{-1}.

Calculations were carried out using Gaussian 03 [11] with the three-parameter hybrid functionals of Becke [12] and the correlation functional of Lee et al. (B3LYP) [13] with a 6-31G* basis set for both carbon and fluorine. This basis set was chosen as a compromise between speed and accuracy of the calculation; the same basis set was used by Kovács and Szabó [8] in a similar theoretical investigation of per-fluorinated adamantane. The geometry was optimised with the Berny algorithm and vibrational frequencies were calculated from the second derivatives of the energy with respect to the Cartesian nuclear coordinates. Raman intensities were calculated by numerical differentiation of dipole derivatives with respect to the electric field.

3. Results

Analogously to the results of Kovács and Szabó for per-fluorinated adamantane [8], the average C–C bond length was found to increase compared with fully hydrogenated triamantane (H-triamantane). For triamantane, this increase was 0.017 Å, greater than the increase for adamantane (0.013 Å). Further, our results showed that the average bond length of the tertiary C–F was larger than that of secondary C–F by 0.013 Å, in agreement with the results of Kovács and Szabó. This change in the C–F bond length occurs because the positive charge on the carbon atom is higher for secondary carbon than tertiary carbon, so the C–F bond length is shorter for secondary carbon [14]. (Note that the calculations are precise to three significant figures, so bond lengths are reported to this level of precision, but it is unlikely that the results are accurate at this level. Therefore, only changes in the bond lengths are reported, rather than absolute bond lengths. Although the difference in the increase of the C–C bond length with fluorination between adamantane and triamantane is small (0.004 Å), the comparison is valid because both were both calculated at the same level of theory.) The F-triamantane molecule had lower symmetry (C_2) than the H-triamantane (C_{2v}), in accordance with a general trend for fluorination to disrupt molecular symmetry.

There is remarkably close agreement between the calculated and experimental Raman spectra (Fig. 2). The experimental spectrum was measured down to 200 cm^{-1}. There are some small peaks in the calculated spectra below this, down to 90 cm^{-1}, but the intensity of these peaks was so small as to be insignificant, so they are not shown in Fig. 2. The r.m.s. deviation between calculated and experimental wavenumber of the vibrations is 4.3 cm^{-1} (compared with 9.9 cm^{-1} reported by Kovács and Szabó [8] for a similar study comparing experimental and calculated vibrational spectra of per-fluorinated adamantane). While the frequencies of the vibrations in the calculated spectrum match closely those in the experimental spectrum, the match between the relative intensities of the peaks is not as good, as has been noted previously for other similar systems [7,15], particularly the ratio of the intensity of the 1300 cm^{-1} peak to the intensities of the 200–700 cm^{-1} peaks. The tendency for the intensity of the ~1300 cm^{-1} peak to be overestimated relative to those at 300–600 cm^{-1} in the calculated spectrum has been previously reported for per-fluorinated adamantane [16].

As for per-F-adamantane [8], the spectrum of the F-triamantane has a strong, broad peak at ~1300 cm^{-1}, with a series of sharper peaks mostly between 200 cm^{-1} and ~500 cm^{-1}. From the results

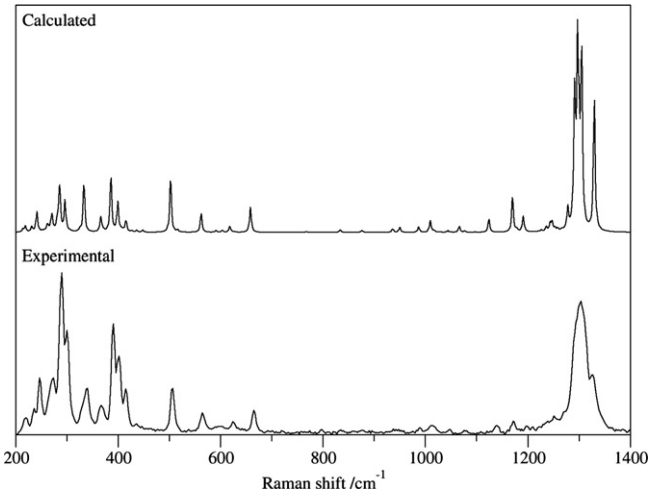

Fig. 2. Calculated and experimental Raman spectra for F-triamantane. The simulated spectrum was generated with Lorentzian functions with a peak width of 2 cm^{-1}; frequencies were not scaled.

of the calculation it can be seen that the broad peak at ~1300 cm^{-1} is composed of several (approximately equally intense) peaks at 1291 cm^{-1}, 1297 cm^{-1} 1305 cm^{-1} and 1329 cm^{-1} as well as a smaller peak at 1300 cm^{-1}. The peak at 1329 cm^{-1} appears as a separate sharp peak in the calculated spectrum but only as a shoulder on the broad peak in the experimental spectrum. The vibrations giving rise to these peaks are discussed below.

As for H-triamantane [15], F-triamantane has 120 vibrational modes ($35A_1 + 24A_2 + 30B_1 + 31B_2$) (an abbreviated list of the vibrations is shown in Table 1; a full list is presented in the Supplementary Material). The calculated spectra for both H-triamantane and F-triamantane are shown in Fig. 3. For H-triamantane, there are several peaks at higher wavenumbers, between 2990 cm^{-1} and 3050 cm^{-1}, corresponding to CH stretching modes, but these are not shown in this paper as we are only interested in a comparison with F-triamantane.

The spectrum of H-triamantane shows many sharp peaks between ~900 cm^{-1} and 1400 cm^{-1}, most of which do not appear in the spectrum of F-triamantane. For H-triamantane, the peaks in this range correspond to strongly mixed CC stretching and CH bending modes [5]. Replacing the hydrogen with fluorine results in a shift in the surface bending modes to lower wavenumbers (between ~200 cm^{-1} and ~500 cm^{-1}) due to the increased mass of the substituent atoms. Similarly, it has been previously reported that an artificial increase in the mass of the hydrogen terminating species from 1 amu to 100 amu in the calculation for H-triamantane causes separation of the bulk stretching modes and the surface atom bending modes, thus removing the peaks associated with mode mixing that are seen between ~1000 and ~1400 cm^{-1} [5,17].

For H-triamantane, vibrations at low wavenumbers are CCC bending modes [15]. For F-triamantane, due to the shifting of the surface bending modes to lower wavenumbers, these surface bending modes are mixed with the CCC bending modes, thus giving rise to a series of peaks at these wavenumbers. For example, animations of an analogous cage deformation (CCC bending) mode

Table 1
Calculated vibrations of F-triamantane

ν_i	Raman shift (cm^{-1})	Symmetry	Raman intensity	ν_i	Raman shift (cm^{-1})	Symmetry	Raman intensity
12	214.0	A_2	1.67	62	603.7	B_2	1.03
13	218.8	A_1	3.48	64	618.3	A_1	2.64
14	231.2	B_2	3.00	66	658.2	A_1	15.3
17	241.2	A_1	12.1	75	876.0	A_1	1.24
23	261.4	A_1	1.15	76	936.0	A_1	1.91
24	262.0	B_2	2.44	77	949.9	A_2	2.97
26	268.3	B_2	1.64	79	986.7	B_2	3.13
27	270.7	A_1	9.45	80	1009.5	A_1	7.23
31	281.1	A_1	4.52	87	1066.2	B_1	3.43
32	282.4	A_1	2.21	92	1124.0	A_1	7.46
33	285.4	B_2	7.67	95	1170.0	A_1	20.5
34	285.9	A_2	19.2	98	1177.6	B_2	1.18
36	296.2	A_1	18.5	101	1191.0	A_1	9.00
41	325.3	B_2	1.39	105	1226.7	B_2	1.11
42	333.2	A_1	28.4	106	1236.0	A_1	2.78
43	365.5	B_1	2.34	108	1243.3	A_1	4.74
44	366.5	B_2	7.13	109	1247.2	B_2	5.20
47	385.7	A_1	32.5	110	1252.6	B_2	1.71
48	399.3	B_1	18.3	111	1258.0	A_1	1.46
49	407.0	A_1	1.29	113	1277.8	A_1	12.8
52	415.4	B_1	6.41	114	1291.2	B_1	79.1
54	436.0	A_1	1.04	115	1296.9	A_1	100.0
56	447.9	B_1	1.11	116	1299.6	B_2	30.3
57	502.3	A_1	31.5	117	1300.6	B_1	10.4
58	516.2	B_2	1.33	118	1304.8	B_2	90.7
59	562.1	A_1	11.0	119	1305.8	A_1	10.3
60	590.9	A_1	1.06	120	1329.7	A_1	79.8

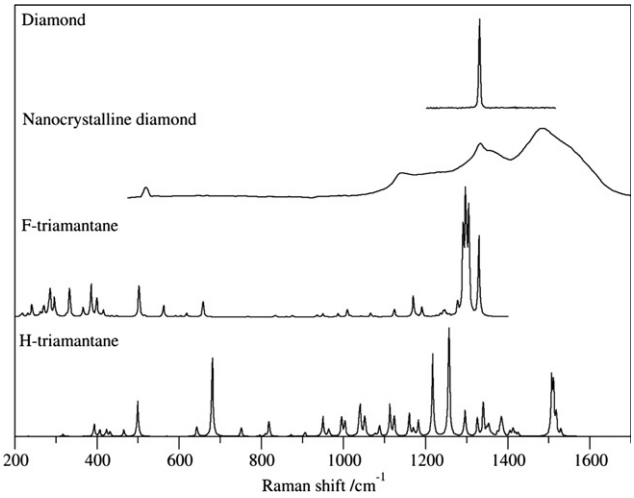

Fig. 3. Calculated spectra for F-triamantane and H-triamantane; for comparison, experimental spectra for nanocrystalline diamond and pure diamond are also shown.

for both H-triamantane and F-triamantane (Supplementary Material) show the increased degree of surface bending that is mixed with the cage deformation for the fluorinated molecule. Due to the mixing with surface bending modes and the relatively high mass of fluorine, the cage deformation is shifted to a lower wavenumber; the deformation giving rise to the peak at 648.6 cm^{-1} for H-triamantane is seen at 261.4 cm^{-1} for F-triamantane.

The surface stretching modes are also shifted to lower wavenumbers when hydrogen is substituted with fluorine, from ~3000 cm^{-1} for H-triamantane to ~800–1300 cm^{-1} for F-triamantane, so for F-triamantane there is mode mixing between the CC and CF stretching modes at wavenumbers between ~800 cm^{-1} and 1300 cm^{-1}. Animations of the same CC stretching mode for both H-triamantane and F-triamantane show the presence of surface bending modes in the case of H-triamantane and CF stretching modes for F-triamantane (Supplementary Material). This mode is seen at 1340.4 cm^{-1} for H-triamantane and 1296.9 cm^{-1} for F-triamantane.

Therefore, the results of this work correspond to the observation of Kovács and Szabó [8], who reported significant mixing of the skeleton and ligand vibrations in fluorinated adamantane due to the similar mass of C and F. Their results show predominantly mixing of CCC bending and surface bending modes at low wavenumbers and mixing of CC and CF stretching modes at higher wavenumbers, in agreement with these new results for F-triamantane.

The net result of the mixing of the CC and CF stretching modes is that, for vibrations at wavenumbers above ~900 cm^{-1}, there is no longer a significant difference in the behaviour of the surface groups and the bonds through the rest of the molecule, so the F-triamantane behaves as if it is a small diamond crystal. Therefore, substituting the hydrogen with fluorine has a similar effect to increasing the mass of the hydrogen terminating species to 100 amu, as was done in the work of Negri et al. [17] and Filik et al. [5] to simulate the effect of confining a small diamond crystal within an amorphous carbon network. Hence, the vibrations observed at these wavenumbers begin to approximate those observed for diamond (i.e. a single strong peak at 1332 cm^{-1} corresponding to the zone-centre mode, Fig. 3), with the only vibrations being a relatively small number of strong stretching modes at ~1300 cm^{-1}. Similarly, Kovács and Szabó [8] observed only a single broad peak at ~1300 cm^{-1} in the experimental Raman spectrum of F-adamantane (determined by calculation to be

composed of several vibrations very close in frequency). When the mass of the hydrogen terminating species of the adamantane derivative $C_{84}H_{64}$ was increased to 100 amu [5], the signal corresponding to the diamond zone-centre mode occurred at 1317 cm^{-1}. For F-triamantane, this signal occurs at 1329 cm^{-1}.

It could be expected that further increases in the mass of the substituent atom would lead to a further decrease in the wavenumber and intensity of peaks in the spectra corresponding to the surface bending modes, along with the further convergence of the CC and surface stretching modes to a single strong peak at $\sim$1300 cm^{-1}. This is in agreement with the predictions of Filik et al. [5], who suggested that surface termination of an adamantane derivative with a heavy substituent, such as bromine, rather than hydrogen, would produce a Raman spectrum very similar to that of diamond.

As the mass of the surface groups increases and the vibrational behaviour of the diamondoid molecule more closely resembles that of a small piece of pure diamond, the differences between the calculated spectrum of the isolated diamondoid molecule and the experimental spectrum for nanocrystalline diamond can be used to distinguish between peaks that are due to diamond nanocrystals and those that are due to defects or grain boundary structures in nanocrystalline diamond. The absence of a peak at $\sim$1150 cm^{-1} in the spectrum of F-triamantane suggests that this peak, which is observed in the vibrational spectrum of nanocrystalline diamond (Fig. 3), is due to such grain boundary structures, rather than to diamond nanocrystals, in agreement with previous studies [5].

4. Conclusions

F-triamantane has been successfully synthesised and the vibrational spectrum reliably reproduced by calculation at the B3LYP/6-31G* computational level. Compared with H-triamantane, the vibrational spectrum more closely resembles that of pure diamond, with stretching modes at $\sim$1300 cm^{-1} dominating the spectrum and the surface bending modes shifted to lower wavenumbers. No peaks were found at $\sim$1150 cm^{-1}, suggesting that the peak at this wavenumber observed in the Raman spectrum of nanocrystalline diamond must be due to grain boundary structures, rather than to vibrations of the diamond nanocrystals.

Acknowledgements

The authors gratefully acknowledge the assistance of Natalie Fey with Gaussian03, James Smith and Keith Rosser for help with the Raman system, and the Ramsay Memorial Fellowships Trust for funding.

Appendix A. Supplementary material

Supplementary material associated with this article can be found, in the online version, at doi:10.1016/j.cplett.2008.06.011.

References

[1] Y. Lifshitz et al., Science 297 (2002) 1531.
[2] M.A. Meador, Ann. Rev. Mater. Sci. 28 (1998) 599.
[3] W.L. Yang et al., Science 316 (2007) 1460.
[4] N.D. Drummond, Nature Nanotechnol. 2 (2007) 462.
[5] J. Filik, J.N. Harvey, N.L. Allan, P.W. May, J.E.P. Dahl, S. Liu, R.M.K. Carlson, Phys. Rev. B 74 (2006).
[6] J.E. Dahl, S.G. Liu, R.M.K. Carlson, Science 299 (2003) 96.
[7] S.L. Richardson, T. Baruah, M.J. Mehl, M.R. Pederson, Chem. Phys. Lett. 403 (2005) 83.
[8] A. Kovacs, A. Szabo, J. Mol. Struct. 519 (2000) 13.
[9] V.Z. Williams, P.V. Schleyer, G.J. Gleicher, L.B. Rodewald, J. Am. Chem. Soc. 88 (1966) 3862.
[10] F.S. Hollowood, M.A. McKervey, R. Hamilton, J.J. Rooney, J. Org. Chem. 45 (1980) 4954.
[11] M.J. Frisch, et al., Gaussian 03, Revision C.02, Gaussian, Inc., Wallingford, CT, 2004.
[12] A.D. Becke, J. Chem. Phys. 98 (1993) 5648.
[13] C.T. Lee, W.T. Yang, R.G. Parr, Phys. Rev. B 37 (1988) 785.
[14] D.L. Cooper, N.L. Allan, R.L. Powell, J. Fluorine Chem. 46 (1990) 317.
[15] J. Filik, J.N. Harvey, N.L. Allan, P.W. May, J.E.P. Dahl, S.G. Liu, R.M.K. Carlson, Spectrochim. Acta A – Mol. Biomol. Spectroscopy 64 (2006) 681.
[16] J. Filik, Ph.D. Thesis, University of Bristol, Bristol, United Kingdom, 2006.
[17] F. Negri, C. Castiglioni, M. Tommasini, G. Zerbi, J. Phys. Chem. A 106 (2002) 3306.